Biomedicine & Pharmacotherapy 85 (2017) 646–657

Available online at
ScienceDirect
www.sciencedirect.com

Elsevier Masson France
EM|consulte
www.em-consulte.com/en

Novel butyrylcholinesterase inhibitors through pharmacophore modeling, virtual screening and DFT-based approaches along-with design of bioisosterism-based analogues

Dhrubajyoti Gogoi[a], Amrita Kashyap Chaliha[b], Diganta Sarma[c], Bibhuti Bhusan Kakoti[a], Alak Kumar Buragohain[b,*]

[a] DBT-Bioinformatics Infrastructure Facility, Centre for Biotechnology and Bioinformatics, School of Science and Engineering, Dibrugarh University, Dibrugarh, Assam, India
[b] Centre for Biotechnology and Bioinformatics, School of Science and Engineering, Dibrugarh University, Dibrugarh, Assam, India
[c] Department of Chemistry, School of Science and Engineering, Dibrugarh University, Dibrugarh, Assam, India

ARTICLE INFO

Article history:
Received 21 May 2016
Received in revised form 16 November 2016
Accepted 16 November 2016

Keywords:
Butyrylcholinesterase (BChE)
Pharmacophore modeling
Molecular docking
ADMET
DFT

ABSTRACT

Ligand and structure-based pharmacophore models were used to identify the important chemical features of butyrylcholinesterase (BChE) inhibitors. A training set of 16 known structurally diverse compounds with a wide range of inhibitory activity against BChE was used to develop a quantitative ligand-based pharmacophore (Hypo1) model to identify novel BChE inhibitors in virtual screening databases. A structure-based pharmacophore hypothesis (Phar1) was also developed with the ligand-binding site of BChE in consideration. Further, the models were validated using test set, Fisher's Randomization and Leave-one-out validation methods. Well-validated pharmacophore hypotheses were further used as 3D queries in virtual screening and 430 compounds were finally selected for molecular docking analysis. Subsequently, ADMET, DFT and chemical similarity search were employed to narrow down on seven compounds as potential drug candidates. Analogues of the best hit were further developed through a bioisosterism-guided approach to further generate a library of potential BChE inhibitors.

1. Introduction

Alzheimer's disease (AD) is the most common cause of dementia, amounting to 50–70% of all such reported cases. AD leads to gradual and severe deterioration of the central nervous system, especially with the onset of middle age, and with the increase in longevity of the average human lifespan, there is increasing incidence of AD in the present times. Dementia has been reported to affect about 47 million people worldwide in 2015, and this figure is set to reach 75 million by 2030. If unchecked, this figure would further escalate to 131 million by 2050, with the maximum of incidence of cases in low-income and middle-income countries [1]. The first mutation detected in familial studies of AD was identified in the ß-amyloid precursor protein (APP) gene on chromosome 21. Missense mutations in the APP gene have been attributed to the development of Early-onset Alzhemer's Disease (EOAD) via an amyloidogenic mechanism. Similar mutations in two other genes, viz., about 80 in presenilin 1 (PS1) and six in presenilin 2 (PS2) till date have also been implicated in a sizeable proportion of familial EOAD cases [2]. Late-onset Alzheimer's disease (LOAD) too has a strong genetic basis and 22 genetic loci have been identified till date that may indicate genetic predisposition for LOAD. APOE is the primary gene implicated for LOAD. Genome-wide association studies (GWAS) have further discerned 21 additional susceptibility loci including BIN1, MEF2C, INPP5D, CD2AP, TREM2, HLA-DRB1/HLA-DRB5, EPHA1, ZCWPW1, NME8, CLU, PTK2B, MS4A6A, CELF1, PICALM, SORL1, SLC2A4, FERMT2, DSG2, CD33, ABCA7 and CASS4 [3].

AD leads to a loss in cholinergic neurons and is associated with the loss in intellectuality of the brain associated with aging [4]. Common progressive dementia, extracellular build-up of β-amyloid proteins to form senile plaque, neuro-fibrillary tangles at proximal dendrites, neuronal dysfunction and death, and synaptic loss are the major neuropathological hallmarks of the disease [5,6].

* Corresponding author at: Dibrugarh University, Dibrugarh, 786004 Assam, India.
E-mail addresses: alakkrburagohain@gmail.com, alak@dibru.ac.in (A.K. Buragohain).

http://dx.doi.org/10.1016/j.biopha.2016.11.076
0753-3322/

Though the cholinergic system is the most affected neurotransmitter system, substantial losses are also sustained in the forebrain, cortex, and hippocampus- all of which play a vital role in the acquisition, processing, and storage of memories of the brain [7]. Cholinergic neurons of the basal forebrain are crucial in modulating other neurotransmitters through extensive cortical projections in the AD brain [1].

AD development is particularly synonymous with a forebrain cholinergic neuron loss and a subsequent progressive decline in Acetylcholine (ACh) levels [2,3]. This has been surmised to be due to increased levels of Acetylcholinesterase (AChE) around the amyloid plaques. A proper elucidation of the relationship between AChE and pathogenesis of AD would only be made possible through extensive research on the various aspects of this topic- though recent studies have reported that both β-amyloid protein and abnormally hyperphosphorylated tau can influence expression of AChE. AChE mediates the cholinergic synapses of the brain and autonomic nervous system by catalyzing the hydrolysis of ACh. AChE selective inhibitors have also been used as AD therapy to amplify the action of ACh at remaining cholinergic synapses in the AD brain. Cholinomimetic drugs are generally prescribed for treatment of AD and centrally acting cholinesterase inhibitors like Tacrin and Donepezil are prescribed as the most effective AD treatment therapy for mild to moderate AD [8]. Only symptomatic treatments are used as therapy for AD- most of them serve to counterbalance the neurotransmitter disturbance, and these come with their fair share of side effects ranging from nausea to possible liver damage [Alzheimers and current therapeutics]. Memantine, an N-methyl-D-aspartate receptor noncompetitive antagonist- is now recommended for treatment of moderate to severe AD but effective treatments by 'disease-modifying' drugs are still to make it to routine therapy for AD [9].

The medicines that are prescribed presently for AD are centrally acting cholinesterases which target both Acetylcholinesterase and Butyrylcholinesterase (BChE). AChE is generally localised in the neurons, whereas BChE is primarily associated with glial cells, endothelial cells, neurons as well as hepatocytes [7]. Various reports concur on the genesis of amyloid protein plaques associated with AD to modification of both AChE and BChE, since cholinesterase inhibitors succeed in diminishing these plaques [27]. BChE activity is however seen to rise progressively in patients with AD whereas that of AChE remains unchanged. The role of BChE in the hydrolysis of ACh towards ameliorating the cholinergic deficiency of the brain, particularly when associated with glia, further strengthen its choice as drug candidate. It has also been reported that at high-level brain activity, local synaptic ACh can reach upto micromolar range in concentration which approach inhibitory levels for AChE activity. Regulation of local ACh levels for maintenance of normal cholinergic function can be credited to the synergistic BChE-mediated hydrolysis brought about by the close spatial relationship of glial BChE. Also, studies on the survival of AChE knockout mice [9] have substantiated the crucial and substitute role of BChE in hydrolysis of ACh [10]. Site-directed mutagenesis and photo-affinity labelling studies of Human BChE establish the independent location and significant difference in ligand-mediated response from that of AChE though they have been assigned similar peripheral sites of binding [2,3]. Thus, BChE is well-supported by independent studies to be forwarded as a biological target for drug discovery studies and has thus been explored in the present study.

Traditional drug discovery and development techniques are time-consuming and resource-demanding processes. Computer-aided drug discovery techniques are hence favoured alternatives to first streamline the processes of drug discovery, design, development and optimization so that only the best hits can be forwarded for further wet lab validation. In the present study, computational techniques such as pharmacophore modeling, molecular docking and Density Functional Theory (DFT) analysis have been performed for identification of potent and selective BChE inhibitors.

2. Materials and methods

2.1. Generation of ligand-based pharmacophore model

HypoGen module of BIOVIA Discovery Studio v4.5 (DS v4.5) was used to generate a 3D ligand-based pharmacophore model from a

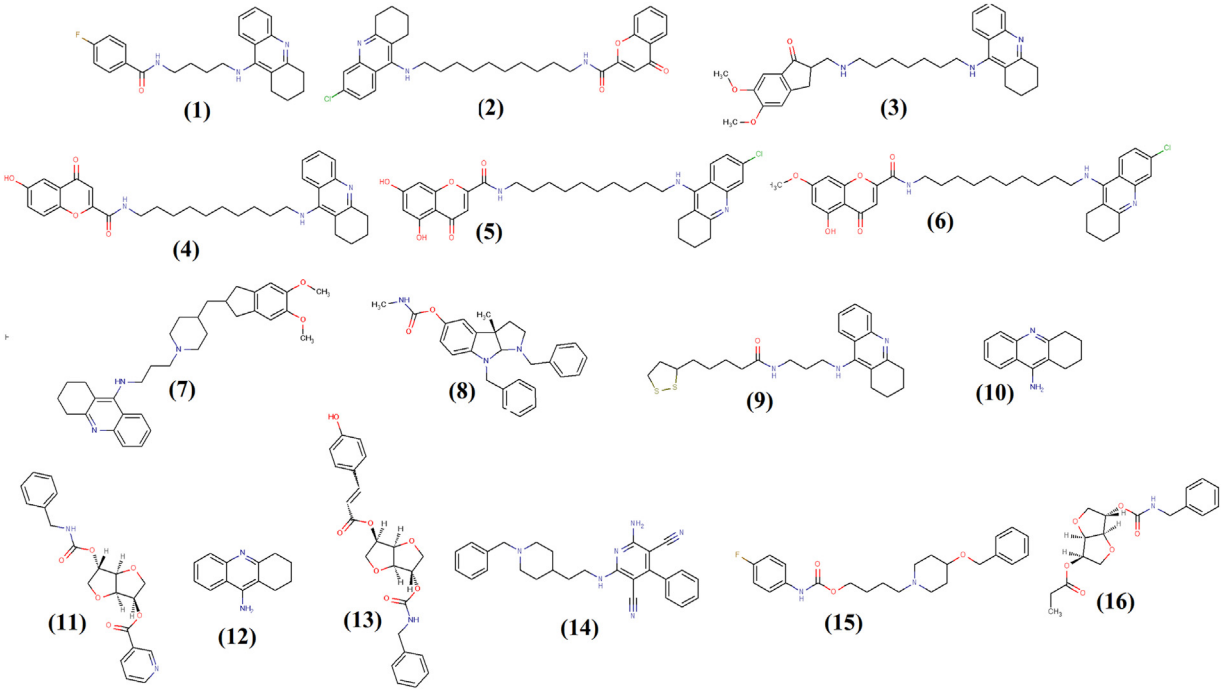

Fig. 1. 2D representation of the training set compounds.

set of known human BChE (BChE; EC 3.1.1.8) inhibitors which were based on a similar type of assay. Ten quantitative pharmacophore hypotheses were generated and the top hypothesis was used as 3D query for virtual screening. Here, we have used 16 structurally diverse chemical entities with activity ranging from 0.035 nmol/L to 980 nmol/L (IC_{50}), ensuring that the activity values are in four orders of magnitude against the human BChE protein. All the compounds and their activity values were retrieved from previous literature and the ChEMBL database [4–9]. Two-dimensional (2D) structures of training set compounds were sketched using MarvinSketch v6.2.0 (ACD Inc., Toronto, Canada) as depicted in Fig. 1 and then converted to 3D form after subjecting them for necessary energy minimization using *Diverse conformation* (DS) software. Dataset compounds were further checked for addition of hydrogen atoms and then minimized using the CHARMM-based smart minimizer that performs 1000 steps of steepest descent followed by conjugate gradient algorithms with a convergence gradient of 0.001 kcal mol^{-1} [10]. DS option was applied and 250 conformations were generated using *BEST* conformer generation protocol of DS which employed the Poling Algorithm at an energy threshold of 15 kcal mol^{-1}. The principle of rigorous energy minimization that is employed in both torsional and cartesian space ensures the best coverage of conformational space by application of the poling algorithm [11,12]. All the 16 compounds were than submitted to the *HypoGen* module of DS v4.5. The minimum and maximum counts for all the features in the hypothesis run were set to 1 and 5 respectively. Uncertainty value was set to 2 and the minimum inter-feature distance was set at 2.5. All other parameters in the *HypoGen* module were kept in default settings [12]. The features that have been considered to develop the pharmacophore model are Hydrogen bond acceptor (HBA), Hydrogen bond donor (HBD), Hydrophobic Aromatic (Hy-Ar), Hydrophobic Aliphatic (Hy-Ali) and Ring Aromatic (AR). Prior to the final hypothesis generation, common features-based pharmacophore (*Feature Mapping*) generation module of DS was used to identify common pharmacophore features among the training set compounds. Best hypothesis (Hypo1) model was analyzed and evaluated based on the cost function and by using determinant factors such as RMSD and correlation between actual versus predicted values of the internal training set compounds.

2.2. Structure-based pharmacophore modeling

Structure-based pharmacophore modeling is a well-established pharmacophore modeling approach which is based on the potential binding sites of known therapeutics to their receptor active sites [13]. Here, we have used the active site of butanoic acid-bound crystal structure of human BChE as a starting point to develop the model. The protein crystal structure was retrieved from Protein Data Bank (PDB code-1P0I) [14]. Prior to hypothesis development, the structure was cleaned and optimized at DS v4.5 workspace. A sphere within a distance of 9 Å from butanoic acid at the binding cavity was selected using the *Edit Binding site prediction tool* of DS. *Interaction generation* protocol of DS was employed to generate the important interaction points corresponding to the catalytically important amino acid residues within the BChE active site [15]. Finally, interaction points were clustered using the *Edit and Cluster* pharmacophore features of DS. Redundant pharmacophoric features were discarded and catalytically important features around the binding cavity were considered for the final model development. Exclusion volumes were then added to the pharmacophore model and the best pharmacophore (Phar1) was built. Phar1 was further validated using a test set and was used as 3D query in the virtual chemical screening.

2.3. Validation and evaluation of Hypo1 and Phar1

Hypo1 was evaluated based on the cost components which were generated during model development. Statistically important parameters such as RMSD and correlation coefficient were calculated by *HypoRefine* module. The best ligand-based pharmacophore model would have high correlation coefficient, low RMSD values and cost components such as total cost would be closer to the fixed cost than to the null cost [10,12]. Hypo1 was validated using the group of test set compounds (Fig. S1 and Table S1 as Supplementary data), Fisher's Randomization and Leave-one-out methods set was prepared based on the 40 structurally diverse known BChE inhibitors with the same activity range as the training set compounds. Fisher's Randomization method was additionally employed on the training set compounds to validate statistical robustness of Hypo1. Nineteen random sheets were generated along with the original hypothesis generation, where the significance level was set at 95% confidence by shuffling the activity values of the training set compounds. Further, the leave-one-out method was employed to establish the efficiency of Hypo1. *HypoGen* module was employed to develop 16 Pharmacophore models by leaving one compound at a time. Correlation coefficient (r) values of all the models were further compared with the original pharmacophore hypothesis (Hypo1) to establish the reliability of Hypo1. The structure-based pharmacophore model- Phar1 was also evaluated and validated by a separate set of test compounds with known BChE inhibitory activity presented along-with as Supplementary data (IC_{50} in nmol/L).

2.4. Virtual screening of databases

Well-validated pharmacophore models (Hypo1 and Phar1) were used as 3D queries to screen 460,695 compounds belonging to diverse type of virtual drug-like databases including an in-house anti-malarial compounds database. The databases screened were ChemBridge (www.chembridge.com), MayBridge (www.maybridge.com), NCI (www.cactus.nci.nih.gov), ChemDiv (www.chemdiv.com), and two specific natural product databases, viz., TCM Database (www.tcm.cmu.edu.tw) and IB Screen Natural Product database (www.ibscreen.com). Compounds were sketched using MarvinSketch v6.2.0 and drug-likeness (compounds following Lipinski's rule of five and Veber's drug-likeness [16,17]) and ADMET descriptors were computed at DS before virtual screening. Hypo1 and Phar1 were used to screen compounds from these databases by using *Best/Flexible Search Protocol* from *Ligand Pharmacophore Mapping* module of DS. Fifty best hits (Best S = 50) of each database based on the Fit value with minimum predicted IC_{50} values were considered for ADMET study.

2.5. ADMET computation

Absorption, Distribution, Metabolism, Excretion and Toxicity (ADMET) parameters were computed for all the screened compounds with maximum fit values and minimum IC_{50} values. ADME properties such as Blood-brain Barrier (BBB) permeability, solubility, Human Intestinal Absorption (HIA), oral bioavailability and hepatotoxicity were predicted for each virtually screened compound by Hypo1 and Phar1 and subjected for protein-ligand docking studies.

2.6. Molecular docking studies

Docking was performed for all the virtual hits using two distant algorithms viz., MolDock (Molegro Virtual Docker, MVD v6.0) and LibDock (DS v4.5). MVD is a molecular docking software which is

based on a differential evolution algorithm- the solution of which takes into account the sum of the intermolecular interaction energy between the ligand and the protein, and the intramolecular interaction energy of the ligand [18]. The docking energy scoring function is based on the modified piecewise linear potential (PLP) and is inclusive of new hydrogen bonding and electrostatic terms [19]. MolDock was set at a maximum iteration of 1500 with a simplex evolution size of 50 and a minimum of 20 runs. The flexibility of the bonds of the ligands and the side chain flexibility of the amino acids in the binding cavity were set with a tolerance of 1.10 and strength of 0.90 for docking simulations. RMSD threshold for multiple cluster poses was computed at <2.00 Å. LibDock is a component of DS v4.5 (BIOVIA Discovery Studio v4.5). Crystal structure of human BChE was retrieved from Protein Databank (PDB ID: 1P0I). Further, the model was energetically optimized using CHARMM force field (Steepest Decent and Conjugate Gradient). The active site of the protein is required to be identified prior to docking analysis. This can be represented as a binding site-specifically, a set of points on a grid that lies on a cavity. The binding site employed in the present study is the Butanoic acid binding site [20]. Two methods are generally considered to define the binding site for the protein- the first based on the shape of the receptor using the "Eraser" algorithm, and the second takes into account the volume occupied by the known ligand positions which are already present in the active site of the protein. For the present study, we have employed the second method to predict the active site of the protein. The docking parameters were validated by docking the co-crystal molecule with the active site of protein. All the hits screened from the virtual screening process were forwarded for the docking analysis, and their binding sites were computed using DS [14]. Docking results were subsequently analyzed based on both the docking scores and the ligand-protein binding interactions with the catalytically important amino acids of the binding site. The best hits were then forwarded for DFT analysis.

2.7. Density functional theory (DFT) analysis

The final hits, along with both the most active and the most inactive compounds in the training set of Hypo1, were considered for DFT analysis. DFT calculation was performed at the DFT module of DS v4.5 by using the Becke3-Lee-Yang-Parr correlation function (B3LYP). The orbital energies of the frontier orbital, viz., Highest Occupied Molecular Orbital (HOMO) and the Lowest Unoccupied Molecular Orbital Energy (LUMO) were computed for all the final hits. These orbital energy values play an important role in terms of electron donor and acceptor properties of a molecule and can thus be utilized to understand the reactivity of a molecule in the active site of the protein. The band energy gap ΔE (LUMO-HOMO) was also computed for all the potentials hits and compared with the training set compounds.

2.8. Chemical similarity search

Chemical similarity search was performed for all the top hits in order to search similar scaffolds for the inhibition of BChE. The best identified inhibitors were used to search for 90% or more structurally similar compounds in PubChem database. Further, compounds were also submitted to SciFinder Scholar and PubMed to ascertain their novelty as BChE inhibitors.

2.9. Design of structural analogues of selected lead compounds

The best scoring compound was further used as the Lead Compound (LC) to develop bioisosteres which would serve as more efficient butyrylcholinesterase inhibitors. Series of analogues were designed by replacing the important side chain of the best hit using molecular replacements acquired from the Swiss Bioisostere database (2012) (www.swissbioisostere.ch).This database is a collection of information on 4.5 million molecular sub-structural replacements and their information in biochemical assays created through detection of matching molecular pairs and by the process of mining bioactivity data in the ChEMBL database [21]. The entire analogue library was then subjected to molecular docking analysis using LibDock of DS.

3. Results and discussion

Ligand and structure-based pharmacophore modeling is used to elucidate the spatial arrangement of chemical features that are

Table 1
Experimental and estimated IC_{50} values of the training set compounds based on best pharmacophore Hypothesis Hypo1.

Name	IC_{50} nmol/L		Error[a]	Activity Scale[b]		Fit Value[c]	Ref.
	Experimental	Estimated		Experimental	Estimated		
Compound 1	0.035	0.017	−2.1	++++	++++	9.94	[8]
Compound 2	0.08	0.5	+6.3	++++	++++	8.47	[6]
Compound 3	0.6	1.2	+2	++++	+++	8.09	[7]
Compound 4	1.5	2	+1.3	+++	+++	7.87	[6]
Compound 5	2.5	3.6	+1.4	+++	+++	7.62	[6]
Compound 6	5	2.6	−1.9	+++	+++	7.75	[6]
Compound 7	7.2	4	−1.8	+++	+++	7.57	[7]
Compound 8	8.1	3.6	−2.3	+++	+++	7.62	[28]
Compound 9	12	24	+2	++	++	6.78	[29]
Compound 10	24	43	+1.8	++	++	6.54	[7]
Compound 11	57	44	−1.3	++	++	6.53	[4]
Compound 12	58	43	−1.4	++	++	6.54	[30]
Compound 13	73	71	−1	++	++	6.32	[4]
Compound 14	670	1200	+1.7	+	+	5.11	[31]
Compound 15	780	310	−2.6	+	+	5.69	[9]
Compound 16	980	480	−2.1	+	+	5.49	[4]

[a] Error value calculated as the ratio of measured activity to estimated activity or the inverse if the estimated activity is greater than the measured activity. Positive value indicates that the estimated IC_{50} is higher than the experimental IC_{50}; negative value indicates that the estimated IC_{50} is lower than the experimental IC_{50} in nmol/L.

[b] Activity scale: $IC_{50} < 1$ nmol/L (Most active, ++++); 1 nmol/L $\leq IC_{50} <$ 10 nmol/L (Active,+++); 10 nmol/L $\leq IC_{50} <$ 100 nmol/L (Moderately Active,++); $IC_{50} \geq$ 100 nmol/L (Inactive, +).

[c] Fit value indicates how well the features in the pharmacophore overlap the chemical features in the molecule. Fit = weight × [max (0, 1-SSE)] where SSE = (D/T)2, where D = displacement of the feature from the centre of the location constraints and T = the radius of the location constraint sphere for the feature (tolerance). The higher the value, the better the fit.

crucial to inhibit biological targets. In the current investigation, a set of known BChE inhibitors was used to develop a quantitative pharmacophore hypothesis in order to identify novel BChE inhibitors from selected chemical databases. A structure-based pharmacophore model was also designed using the BChE active site and subjected for virtual screening of chemical databases.

3.1. Ligand and structure-based pharmacophore model generation

Ten ligand-based pharmacophore models were developed from a training set of 16 compounds with inhibitory activity against BChE in nmol/L concentration (Table 1). Structures of the training set compounds are depicted in Fig. 1, and the statistical factors such as cost, correlation coefficient (r), and RMSD for each hypothesis have been enumerated in Table 2. According to the Debnath analysis [22], the best hypothesis should have the highest cost difference, a good correlation co-efficient, the least RMSD, and a significant total cost value. Cost difference and configuration cost are the determinants in identification of top pharmacophore hypotheses. Cost difference is the difference between the null and total cost. A 40–60 bit difference is assumed to have a predicted correlation probability of 75–90% and a difference greater than 60-bit is assumed to have a predicted correlation probability of more than 90%. Here, the top hypothesis Hypo1 has a cost difference of 40–60 bits that amounts to a value of 112.413 bits and suggests a chance of representing a significant correlation in the data [10,12].

Hypo1 shows the highest correlation coefficient of 0.968 and thus establishes its superior predictive capacity in comparison to Hypo 2, Hypo 3 and Hypo10. Correlation coefficient is based on the linear regression derived from geometric fit index. RMS value is the deviation of the predicted activity value from the experimental value. The RMS values of Hypo1, Hypo2 and Hypo3 are 1.066, 1.259 and 1.279 respectively. Minimum RMS value of Hypo1 is significant and thus supports the novelty of the hypothesis [20]. Reliability of Hypo1 also depends on whether the total cost value is distant from the null cost and close to the fixed cost. Here, Hypo1 shows the total and null cost scores to be 77.179 and 189.592 respectively. Configuration cost is another important cost function to analyze the reliability of pharmacophore hypothesis and the configuration cost of a hypothesis is required to be less than 17 for a statistically significant model. The configuration cost has been found to be 16.79 which support Hypo1 as a novel hypothesis. Having satisfied all requirements of a good hypothesis, Hypo1 was finally identified as the best ligand-based hypothesis to be used as 3D query in virtual screening. Hypo1 consisted of two Hydrogen Bond Acceptor features (HBA), one Hydrogen Bond Donor (HBD), one Hydrophobic-Aliphatic (Hy-Ali) feature and one Ring Aromatic (RA) feature. The chemical features and 3D spatial arrangement of Hypo1 are shown in Fig. 2.

Table 2
Results of top pharmacophore hypotheses by *HypoGen* Algorithm.

Hypothesis	Total Cost	Cost Difference[a]	RMSD	Correlation	Features	Max Fit
Hypo1	77.179	112.413	1.066	0.968	*HBA, HBD, Hy-Ali, RA*	10.224
Hypo2	79.557	110.035	1.259	0.954	*HBD, Hy-Ali, 2Hy-Ar, AR*	8.538
Hypo3	80.297	109.295	1.279	0.953	*HBD, Hy-Ali, 2AR*	9.533
Hypo4	80.937	108.655	1.155	0.963	*HBA, HBD, Hy-Ar, RA*	11.359
Hypo5	80.966	108.626	1.302	0.951	*HBD, Hy-Ali, Hy-Ar, RA*	9.717
Hypo6	80.980	108.612	1.338	0.948	*HBD, Hy-Ali, Hy-Ar, RA*	8.910
Hypo7	84.725	104.867	1.508	0.934	*HBA, HBD, Hy-Ar, RA*	8.633
Hypo8	85.357	104.235	1.529	0.932	*HBA, Hy-Ali, 2Hy-Ar, RA*	8.934
Hypo9	85.964	103.628	1.540	0.931	*2HBA, Hy-Ali, 2Hy-Ar*	9.322
Hypo10	88.167	101.425	1.636	0.922	*2HBA, Hy-Ali, 2Hy-Ar*	8.719

Null Cost = 189.592, Fixed Cost = 88.167, Configuration Cost = 16.79.
[a] Cost difference = null cost-total cost; abbreviation used for features: HBA, hydrogen-bond acceptor; HBD, hydrogen-bond donor; Hy-Ali, Hydrophobic Aliphatic; Hy-Ar, Hydrophobic Aromatic; RA, Ring Aromatic.

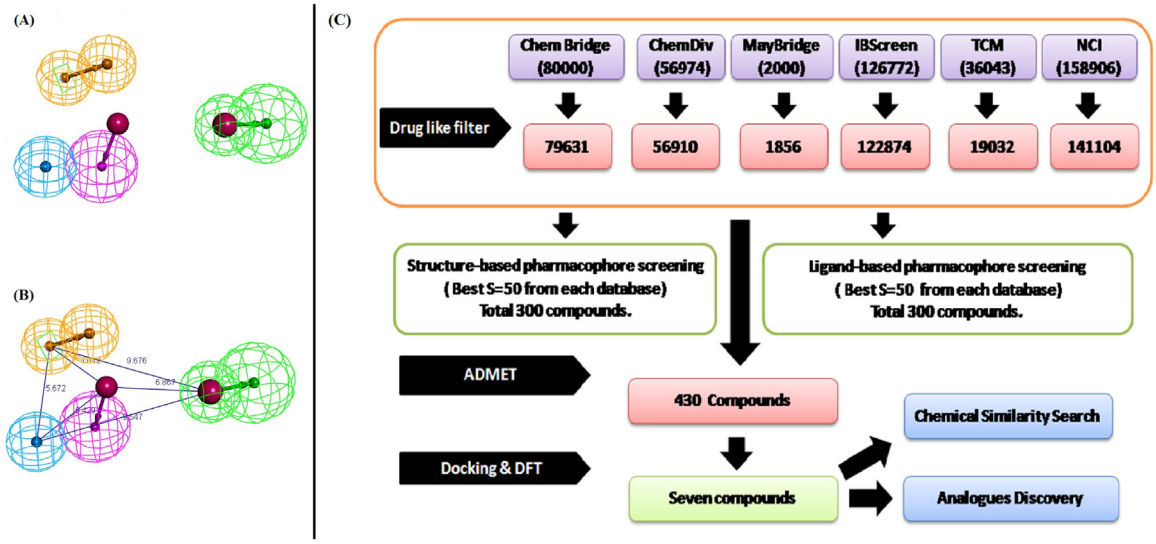

Fig. 2. Best HypoGen pharmacophore model Hypo1: (A) chemical features of Hypo1 (B) geometric parameters of Hypo1 (C) flowchart depicting the virtual screening process employed in this study.

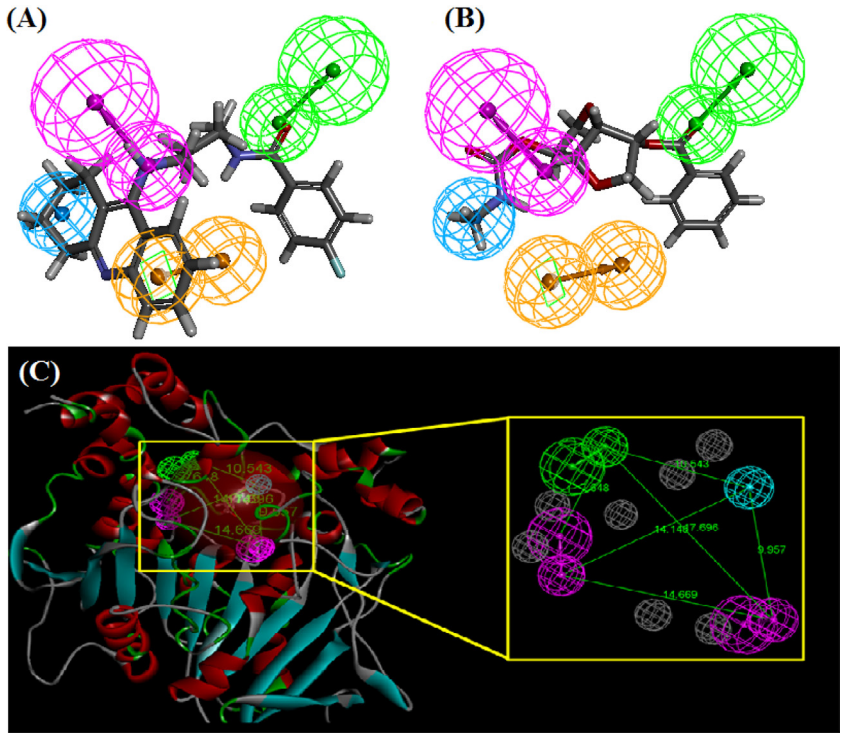

Fig. 3. Overlay of Most Active (A) and Most inactive compound (B) of the training set compounds on the Hypo1; Spatial features of Phar1 (Structure-based Pharmacophore hypothesis) in the active site of BChE receptor model (C).

Hypo1 was used to estimate the inhibitory activity of 16 internal training set compounds to elucidate its predictive power in identifying potential BChE inhibitors and was found to be able to predict the inhibitory activity values of the 16 training set compounds in the same order of magnitude except Compound 3 (Table 1), which was underestimated by Hypo1 as moderately active. Hypo1 aligned to most active (0.035 nmol/L) and most inactive compounds (980 nmol/L) as depicted as Fig. 3. The correlation plot of estimated versus and predicted values in logarithmic scale has been shown in Supplementary data, Fig. S2. Analysis of these results established Hypo1 as a remarkable pharmacophore model with minimum error.

3.2. Structure-based pharmacophore modeling

Structure-based pharmacophore hypothesis (Phar1) is comprised of six pharmacophoric features (Fig. 3). Phar1 consists of three Hy features, two HBD features and one HBA feature. In addition to these features seven exclusion volume spheres were also taken into consideration to establish the model. All pharmacophoric features are around the active site of butanoic acid of the BChE receptor model. Hence, compounds mapping on some of these identified features may have the potential to inhibit BChE with considerable efficiency.

3.3. Validation of pharmacophore hypothesis

Hypo1 and Phar1 were both validated using standard methods to confirm their predictive efficiency. Hypo1 was validated using a test set of known BChE inhibitors with the same order of activity range as in training set compounds. The test set comprised of 40 such compounds retrieved from literature and were used to examine the ability of Hypo1 in the same activity range. Except for one compound (underestimated as active compound), all the test set compounds have been predicted to be in their own activity range by Hypo1 (Table 3). It showed the correlation co-efficient (r) of 0.94 between the actual and predicted BChE inhibitory activity for the test set (Supplementary data, Fig. S2). This result implies that Hypo1 was not only efficiently predicting the inhibitory activity of the internal training set compounds but was also able to perform the same for the external test set molecules. This validates Hypo1 as a significant pharmacophore model.

Phar1 was also validated using a separate test set of 20 known BChE inhibitors as given in the Supplementary data, Table S2. Test set molecules were retrieved from literature with their activity values and Phar1 was used to screen them using *Screen ligand* option of DS v4.5. Test set compounds were found to map to 2–3 features by Phar1. Hence, Phar1 was validated to be a reliable pharmacophore model to identify potential BChE inhibitors in the virtual screening databases.

Fisher's randomization test was further applied to Hypo1 in order to confirm the hypothesis. Here, 95% confidence level was chosen, and 19 random spreadsheets were developed to produce a random hypothesis (Table S3 as Supplementary data). Further, the random hypotheses thus generated were compared with the original hypothesis. The result of this test also supported the novelty Hypo1 as a true hypothesis.

3.4. Virtual screening

Well-validated hypotheses, Hypo1 and Phar1 were further used as 3D pharmacophore queries for retrieving novel candidate molecules from six databases of drug-like compounds. Of these, two are natural product databases. The reason for consideration of natural product databases is that compounds which have a biological origin are generally seen to have minimum side effects as candidate drugs. Here, we have screened a total of 600 compounds from 460695 database compounds which displayed

Table 3
Experimental and estimated IC_{50} values of the test set compounds based on best pharmacophore hypothesis Hypo 1.

Name	IC_{50} nmol/L		Error[a]	Activity Scale[b]		Ref.
	Experimental	Estimated		Experimental	Estimated	
Compound 1	0.0212	0.041	1.958	++++	++++	[8]
Compound 2	0.038	0.008	−4.467	++++	++++	[6]
Compound 3	0.1	0.017	−5.868	++++	++++	[6]
Compound 4	0.139	2.068	14.882	++++	++++	[32]
Compound 5	0.141	0.053	−2.630	++++	++++	[32]
Compound 6	0.15	0.0185716	−8.076	++++	++++	[6]
Compound 7	0.293	0.155152	−1.888	++++	++++	[32]
Compound 8	0.523	0.0779519	−6.709	++++	++++	[32]
Compound 9	0.969	0.0676563	−14.322	++++	++++	[32]
Compound 10	1.68	0.315104	−5.331	+++	++	[32]
Compound 11	3.4	27.2468	8.013	+++	++	[33]
Compound 12	8.06	1.41006	−5.716	+++	+++	[7]
Compound 13	12.3	28.6509	2.329	++	+++	[7]
Compound 14	21.4	147.545	6.894	++	+	[34]
Compound 15	25	7.25098	−3.447	++	+++	[35]
Compound 16	25.2	21.1568	−1.191	++	++	[36]
Compound 17	31.6	31.173	−1.013	++	+++	[36]
Compound 18	51.29	90.1351	1.757	++	++	[37]
Compound 19	66.3	16.0304	−4.135	+++	+++	[7]
Compound 20	72.69	24.5482	−2.961	+++	+++	[7]
Compound 21	96	132.91	1.383	++	++	[38]
Compound 22	137	18.8227	−7.278	++	+++	[39]
Compound 23	144	1660.55	11.532	+	+	[40]
Compound 24	189	98.3994	−1.920	+	+	[39]
Compound 25	287	357.464	1.245	+	+	[38]
Compound 26	330	803.294	2.434	+	+	[41]
Compound 27	360	1304.11	3.622	+	+	[30]
Compound 28	470	5666.57	12.057	+	+	[36]
Compound 29	542	206.278	−2.627	+	+	[38]
Compound 30	641	375.381	−1.707	+	+	[42]
Compound 31	776	122.724	−6.323	+	+	[28]
Compound 32	800	1255.1	1.568	+	+	[43]
Compound 33	958	5962.43	6.223	+	+	[44]
Compound 34	1300	628.313	−2.069	+	+	[35]
Compound 35	1750	6306.34	3.603	+	+	[41]
Compound 36	2080	10868.4	5.225	+	+	[43]
Compound 37	2250	1260.29	−1.785	+	+	[43]
Compound 38	2470	3105.97	1.257	+	+	[43]
Compound 39	3300	1015.72	−3.248	+	+	[45]
Compound 40	4700	8710.31	1.958	+	+	[45]

[a] Positive value indicates that the estimated IC_{50} is higher than the experimental IC_{50}; negative value indicates that the estimated IC_{50} is lower than the experimental IC_{50} in nmol/L.
[b] Activity scale: $IC_{50} < 1$ nmol/L (Most active, ++++); 1 nmol/L $\leq IC_{50} <$ 10 nmol/L (Active,+++); 10 nmol/L $\leq IC_{50} <$ 100 nmol/L (Moderately Active,++); $IC_{50} \geq$ 100 nmol/L (Inactive, +).

maximum fit to Hypo1 and Phar1 as depicted in Fig. 2. Prior to virtual screening, all selected database compounds were predicted for drug-likeness properties (Lipinski's and Veber's rule) to minimize the database to a drug-likeness optimized library. We have finally selected 430 compounds with optimum ADME parameters such as BBB penetration, solubility, Cytochrome p450 (CYP50) inhibition, 2D6 inhibition, hepatotoxicity, Human Intestinal Absorption (HIA), Plasma Protein Binding (PPB) (Fig. S2, Supplementary data). These 430 compounds were then forwarded for molecular docking computation.

3.5. Molecular docking

Molecular docking is a well-established method to predict the molecular-level interactions of small molecules in the receptor binding cavity of biological targets. The 3D structure of BChE

Table 4
Docking results of best hits.

Sl No.	Name	DS v4.5	MVD v6.0			Interacting amino acids
		LibDock Score	MolDock Score	Rerank Score	H-Bond	
1	ZINC85569406	151.715	−174.284	−149.41	−13.826	Phe329, Gly116, Trp82, His438, Ser28, Gly117, Trp231, Leu286
2	CB2	150.235	−124.132	−99.7694	−6.644	Pro84, Tyr332, Ser198, Gly438, Trp82, Gly115, Asp70, Phe329, Ala328
3	ZINC58594092	148.614	−163.261	−136.001	−4.847	Ile69, Asp70, Gly117, His438, Ser198, Phe329, Leu286, Trp231
4	CB4	141.41	−132.109	−106.583	−0.692	Gly117, Gly116, Glu97, Phe329, Trp231, Leu286, Phe398, Trp82, Thr120, Gly115
5	ZINC14927255	140.131	−145.624	−114.589	−8.299	Gly78, Ser79, His438, Ser198, Asn83, Gly116, Gly117, Trp231
6	ZINC01408178	139.213	−174.752	−120.475	−0.453	His438, Ala328, Trp82, Trp231, Gly439, Asp70, Leu286
7	ZINC85569423	151.554	−160.088	−133.993	−3.908	Asp70,Asn289, Tyr332, Pro285, Phe329, Ala328, His438

Table 5
Orbital energy value of hits and training set compounds.

Name	LUMO Energy (kcal/mol)	HOMO Energy (kcal/mol)	Band Energy Gap ΔE (LUMO-HOMO)
ZINC58594092	0.0148	−0.055	0.069
ZINC01408178	−0.275	−0.368	0.093
ZINC85569406	−0.2141	−0.329	0.115
ZINC14927255	−0.047	−0.197	0.150
Most active Compound	−0.0499	−0.212	0.160
CB4	0.0008	−0.164	0.164
ZINC85569423	−0.052	−0.221	0.169
CB2	−0.0042	−0.183	0.178
Least active Compound	0.0003	−0.2439	0.244

complexed with Butanoic Acid was acquired from Protein Data Bank [14]. Prior to docking, the protein model was optimized using Steepest Descent and Conjugate Gradient CHARMM based force fields. Docking was performed using two distant algorithms, viz., MolDock and LibDock. Consensus docking scores such as LibDock, MolDock, Rerank and H-Bond energy values were computed and compared with those of the co-crystal ligand. Molecular docking was performed on the butanoic acid binding site of BChE after initially verifying the ability of this co-crystal ligand using the selected parameters to produce the most suitable binding

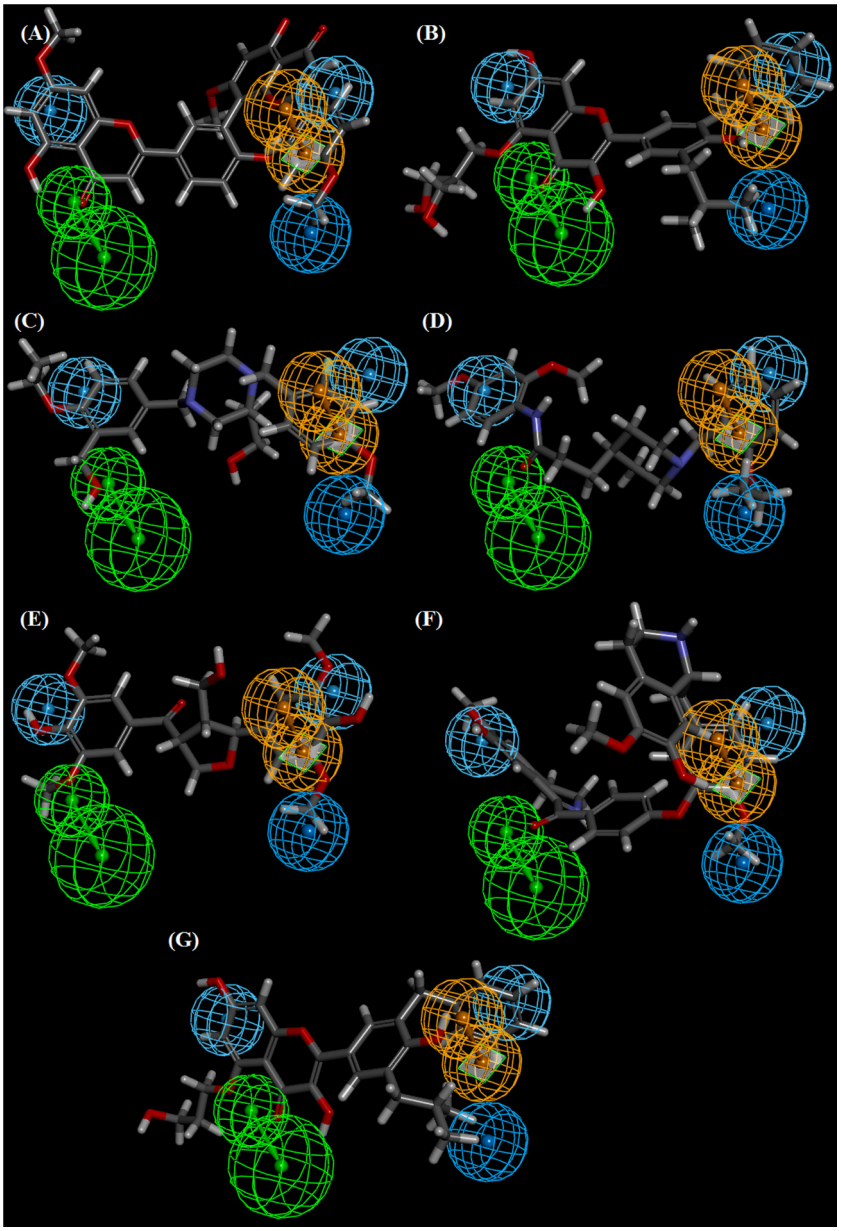

Fig. 4. Overlay of Hypo1 on the best hits- (A) ZINC58594092 (B) ZINC85569406 (C) CB2 (D) CB4 (E) ZINC14927255 (F) ZINC01408178 and (G) ZINC85569423.

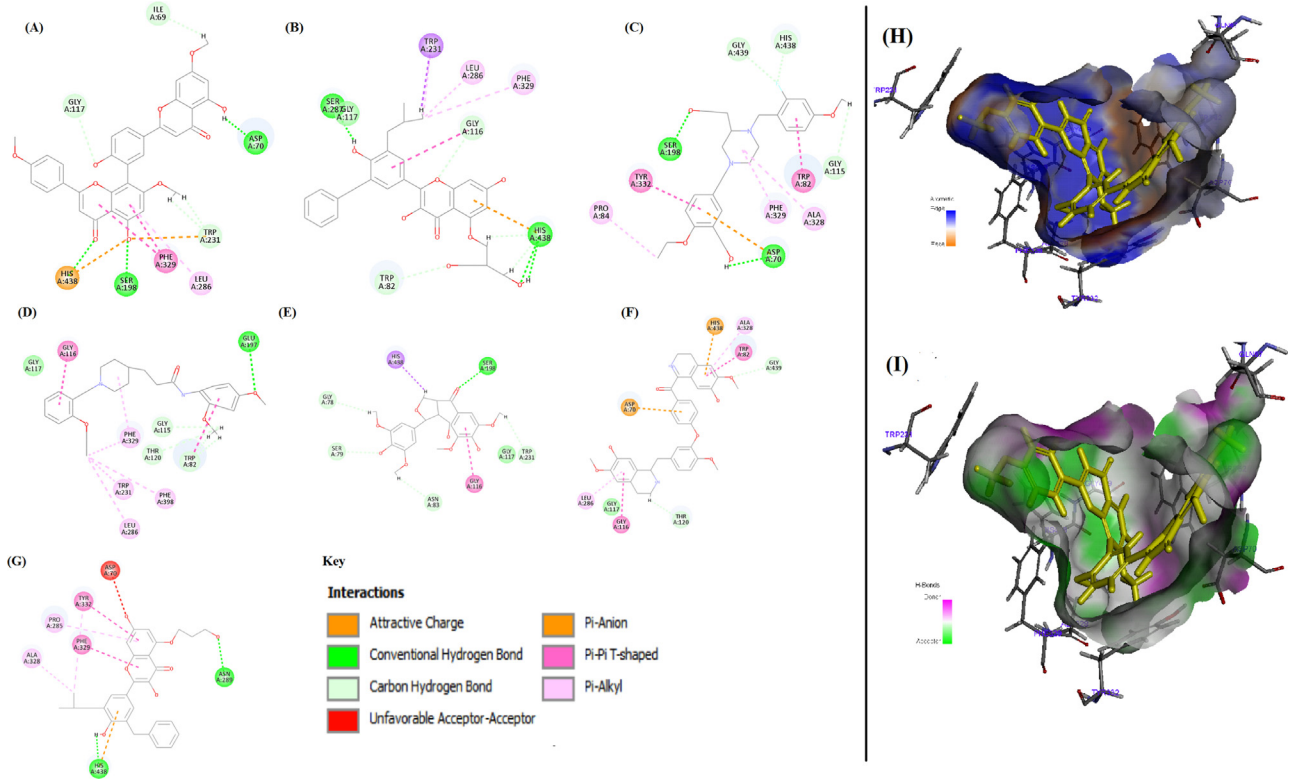

Fig. 5. 2D docking Interaction plots of best hits at the BChE active site – (A) ZINC58594092 (B) ZINC85569406 (C) CB2 (D) CB4 (E) ZINC14927255 (F) ZINC01408178 and (G) ZINC85569423, (H) Aromatic Edge/Face surface and (I) Hydrogen bond donor/acceptor of ZINC58594092 (best hit) binding site.

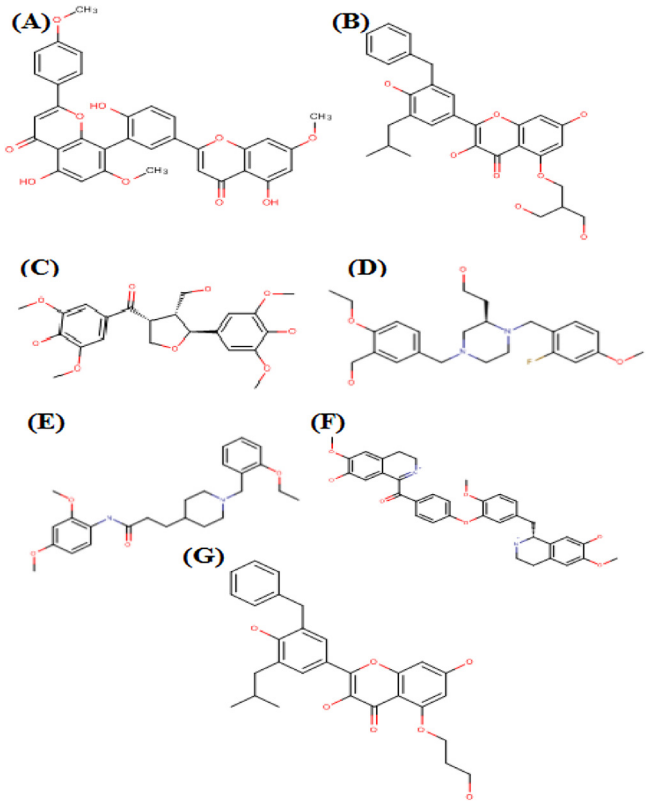

Fig. 6. A 2D representation of the seven final hit compounds – (A) ZINC58594092 (B) ZINC85569406 (C) CB2 (D)CB4 (E) ZINC14927255 (F) ZINC01408178 and (G) ZINC85569423.

orientation [20]. After validation of the same, the same parameters were employed to dock the candidate compounds onto the active site of the protein. The top-ranked 29 compounds based on the highest docking scores were consequently selected to be forwarded as the best potential inhibitors to be forwarded for docking analysis [14]. Of these 29 final hits, 11 compounds were screened by Hypo1 and the remaining 18 compounds were screened from Phar1. Docking results of the selected hits have been presented in Table 4. Significant interactions of all the hits were observed with the crucially located Leu286 of the acyl pocket of the BChE active site- which has been established by previous studies to contribute to substrate specificity and which thus establishes the selectivity of the selected hits for the target enzyme [14].

3.6. Density functional theory (DFT)

HOMO and LUMO are responsible for charge transfer in chemical reactions and hence can be used to analyze the energy transfer and stability of small molecules in the active site of BChE protein [20,23]. The HOMO and LUMO energy values were computed and the energy difference (band energy gap) ΔE (LUMO-HOMO) was then derived to understand the reactivity at molecular level. A low band energy gap is predictive of a reactive compound while a wide energy gap implies that the activity is not sufficient at the active site of a protein receptor [24]. On the basis of the band energy gap, seven compounds were identified as presented in Table 5 and Fig. 7- the ΔE values of which were lower than the most active (ΔE = 0.1602) compound in the training set data.

Mapping of top hits to Hypo1 is depicted in Fig. 4. Of all the proposed hits, the compound ZINC58594092 was found to be the most suitable drug candidate as it satisfied all necessary criteria to be a potent BChE inhibitor. ZINC58594092 was found to interact

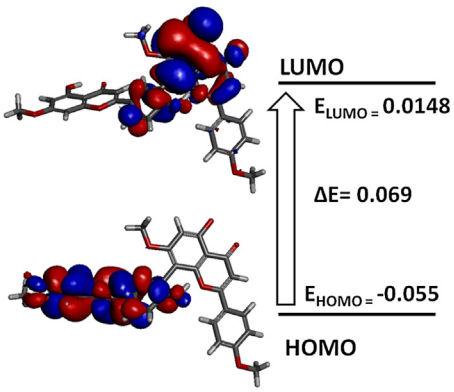

Fig. 7. The orbital energy values and energy gap for compound ZINC58594092.

with amino acids Ile69, Asp70, Gly117, His438, Ser198, Phe329, Leu286 and Trp231 via eight different interactions. It formed two hydrogen bonds with Asp70 and Ser198, three carbon-hydrogen bonds with Ile69, Gly117 and Trp231, and was also observed in the binding orientation of ZINC58594092. Further, two pi-pi and pi-alkyl interactions with Phe329 and Leu286 were also predicted. An attractive charge bond was observed with His438 as depicted in Fig. 5. The 2D representation of best hits along with ZINC58594092 has been presented in Fig. 7. The atomic orbital composition of ZINC58594092 has been displayed in Fig. 6. ZINC58594092 also had the least band energy gap of 0.069 and thus was strongly supported to have a strong inhibitory activity in the BChE active site. The novelty of the six best hits was verified by using PubChem and ChEMBL databases for Chemoinformatics studies. Since compound ZINC58594092 was predicted as the best lead molecule with the most potential to be forwarded as a candidate drug, it was subsequently subjected for chemical similarity search and design of structural analogues.

3.7. Chemical similarity search and development of analogues

The best hit ZINC58594092 was further submitted to the PubChem database to identify structurally similar compounds. The chemical similarity search resulted in 320 compounds, which were 95% or more similar to the best hit. In order to develop more potentially reactive BChE inhibitors, a series of bioisostere-based analogues of ZINC58594092 were designed using the Swiss Bioisostere database. Finally, ten analogues were developed and forwarded for docking studies (Supplementary data). Best analogues of ZINC58594092 have been shown in Fig. S5.

4. Discussion

BChE is imperative in mediating the central cholinergic transmission in healthy neurological functioning. Abnormal expression of BChE is associated with the anomalous neurological conditions collectively referred to as the AD brain. Therefore, its association with the progression of neuropathological changes makes it a justifiable target for treatment of AD. This may be achieved through the mechanism of ameliorating the cholinergic deficiency of the brain [8].

The current medicines that are prescribed for treatment of mild to moderate AD include Rivastigmine, Tacrine, Huperzine A. However, treatment with these medicines are rife with common complaints from side effects which include, but are not limited to, nausea, loss of appetite, increased frequency of bowel movement, GI side effects, possible liver damage etc [12–14]. The present study involved a novel computational approach towards identification of potential BChE inhibitors as alternatives to the present batch of medicines which primarily target AChE, and thus aim to significantly reduce the side-effects normally associated with the same. These candidate molecules could be further subjected to drug development and forwarded as better alternatives to the current batch of medicines used for the treatment of AD.

Though indicated along with AChE to be responsible for the progression of AD, previous research shows that BChE has crucial differences with the AChE target which can be used to selectively inhibit BChE by potential drug candidates. One of these differences is the constitution of the hydrophobic residues lining the gorge of the pocket in BChE, while in AChE the same residues consist of aromatic groups of compounds. Furthermore, the presence of the amino acids Leu286 and Val288 in the acyl-binding pocket of BChE in lieu of Phe288 and Phe290 in that of AChE, as well as the difference of the conformation of the acyl loops in both of these enzymes further establishes the selectivity of potential drug candidates towards BChE [14,25,26].

In the present report, ligand and structure-based pharmacophore models were developed to identify potential and selective BChE inhibitors. The best ligand-based pharmacophore model (Hypo1) consisted of four features (HBA, HBD, Hy-Ali and RA). Same features were also considered for the discovery of novel inhibitors while employing this pharmacophore model approach in previous reports [18]. Hypo1 was evaluated and validated using standard protocols such as test set, Fisher's Test and Leave-one-out methods to confirm its predictive power in identifying novel BChE inhibitors. Hypo1 also exhibited a high correlation coefficient of 0.968 in predicting IC50 values of training set data. A well-validated structure-based pharmacophore model (Phar1) was also developed from the active site of the crystal structure of BChE.

Both models Hypo1 and Phar1 were used as 3D queries in the virtual screening process. Subsequently, compounds with suitable drug-likeness properties and optimum ADMET values were subjected for docking studies using MVD and LibDock docking softwares. LibDock has been reported to perform at par with docking programs that use genetic/growing/Monte Carlo driven algorithms [27]. Based on both docking analysis and ligand-protein interaction study, 29 compounds were selected as potential hits. Significant interactions of the hits were observed with the crucially located Leu286 of the acyl pocket of the BChE active site- which along with Val288, has been established by previous studies to contribute to substrate specificity and which thus establishes the selectivity of the selected hits for the target enzyme [14].

Density functional theory (DFT) is a computational quantum mechanical modelling technique used in the physical sciences to probe the electronic structure of atoms, molecules, and the condensed phases. Frontier orbital energies, viz., HOMO and LUMO were used to calculate the band gap energy which was subsequently employed to ascertain the strength and stability of the molecular interactions. Seven compounds with minimum band gap energy (ΔE = LUMO-HOMO) were finally identified as potential inhibitors of BChE. The top hit ZINC58594092 was identified on the basis of obtaining top scores in all the virtual screening parameters involved in the present investigation. It was hence chosen for further chemical similarity search and the development of bioisostere-based structural analogues.

Conflict of interest

The authors report no declarations of interest.

Acknowledgements

Authors thankfully acknowledge Department of Biotechnology, Govt. of India for providing the Bioinformatics Infrastructure Facility (BIF) at the Centre for Studies in Biotechnology, Dibrugarh University in which the presented work has been performed. Authors also acknowledge Dr. R. L. Bezbaruah, Ex Chief Scientist and Coordinator, DBT-BIF, CSIR-NEIST, Jorhat, Assam for advice and support.

References

[1] H. Noedl, Y. Se, K. Schaecher, B.L. Smith, D. Socheat, M.M. Fukuda, C. Artemisinin Resistance in Cambodia 1 Study, Evidence of artemisinin-resistant malaria in western Cambodia, N. Engl. J. Med. 359 (24) (2008) 2619–2620.
[2] F. Ahmed, R.M. Ghalib, P. Sasikala, K.K. Ahmed, Cholinesterase inhibitors from botanicals, Pharmacogn. Rev. 7 (14) (2013) 121–130.
[3] F. Nachon, L. Ehret-Sabatier, D. Loew, C. Colas, A. van Dorsselaer, M. Goeldner, Trp82 and Tyr332 are involved in two quaternary ammonium binding domains of human butyrylcholinesterase as revealed by photoaffinity labeling with [3H]DDF, Biochemistry 37 (29) (1998) 10507–10513.
[4] C.G. Carolan, G.P. Dillon, J.M. Gaynor, S. Reidy, S.A. Ryder, D. Khan, J.F. Marquez, J.F. Gilmer, Isosorbide-2-carbamate esters: potent and selective butyrylcholinesterase inhibitors, J. Med. Chem. 51 (20) (2008) 6400–6409.
[5] T. Sauvaitre, M. Barlier, D. Herlem, N. Gresh, A. Chiaroni, D. Guenard, C. Guillou, New potent acetylcholinesterase inhibitors in the tetracyclic triterpene series, J. Med. Chem. 50 (22) (2007) 5311–5323.
[6] M.I. Fernandez-Bachiller, C. Perez, L. Monjas, J. Rademann, M.I. Rodriguez-Franco, New tacrine-4-oxo-4H-chromene hybrids as multifunctional agents for the treatment of Alzheimer's disease, with cholinergic, antioxidant, and beta-amyloid-reducing properties, J. Med. Chem. 55 (3) (2012) 1303–1317.
[7] P. Camps, X. Formosa, C. Galdeano, T. Gomez, D. Munoz-Torrero, M. Scarpellini, E. Viayna, A. Badia, M.V. Clos, A. Camins, M. Pallas, M. Bartolini, F. Mancini, V. Andrisano, J. Estelrich, M. Lizondo, A. Bidon-Chanal, F.J. Luque, Novel donepezil-based inhibitors of acetyl- and butyrylcholinesterase and acetylcholinesterase-induced beta-amyloid aggregation, J. Med. Chem. 51 (12) (2008) 3588–3598.
[8] P. Szymanski, A. Karpinski, E. Mikiciuk-Olasik, Synthesis, biological activity and HPLC validation of 1,2,3,4-tetrahydroacridine derivatives as acetylcholinesterase inhibitors, Eur. J. Med. Chem. 46 (8) (2011) 3250–3257.
[9] Y.E. Kwon, J.Y. Park, K.T. No, J.H. Shin, S.K. Lee, J.S. Eun, J.H. Yang, T.Y. Shin, D.K. Kim, B.S. Chae, J.Y. Leem, K.H. Kim, Synthesis, in vitro assay, and molecular modeling of new piperidine derivatives having dual inhibitory potency against acetylcholinesterase and Abeta1-42 aggregation for Alzheimer's disease therapeutics, Bioorg. Med. Chem. 15 (20) (2007) 6596–6607.
[10] S. John, S. Thangapandian, M. Arooj, J.C. Hong, K.D. Kim, K.W. Lee, Development, evaluation and application of 3D QSAR Pharmacophore model in the discovery of potential human renin inhibitors, BMC Bioinf. 12 (Suppl. 14) (2011) S4.
[11] M. Arooj, S. Thangapandian, S. John, S. Hwang, J.K. Park, K.W. Lee, 3D QSAR pharmacophore modeling, in silico screening, and density functional theory (DFT) approaches for identification of human chymase inhibitors, Int. J. Mol. Sci. 12 (12) (2011) 9236–9264.
[12] M. Niu, F. Dong, S. Tang, G. Fida, J. Qin, J. Qiu, K. Liu, W. Gao, Y. Gu, Pharmacophore modeling and virtual screening for the discovery of new type 4 cAMP phosphodiesterase (PDE4) inhibitors, PLoS One 8 (12) (2013) e82360.
[13] S. Thangapandian, S. John, S. Sakkiah, K.W. Lee, Potential virtual lead identification in the discovery of renin inhibitors: application of ligand and structure-based pharmacophore modeling approaches, Eur. J. Med. Chem. 46 (6) (2011) 2469–2476.
[14] Y. Nicolet, O. Lockridge, P. Masson, J.C. Fontecilla-Camps, F. Nachon, Crystal structure of human butyrylcholinesterase and of its complexes with substrate and products, J. Biol. Chem. 278 (42) (2003) 41141–41147.
[15] J. Fei, L. Zhou, T. Liu, X.Y. Tang, Pharmacophore modeling, virtual screening, and molecular docking studies for discovery of novel Akt2 inhibitors, Int. J. Med. Sci. 10 (3) (2013) 265–275.
[16] C.A. Lipinski, F. Lombardo, B.W. Dominy, P.J. Feeney, Experimental and computational approaches to estimate solubility and permeability in drug discovery and development settings, Adv. Drug Deliv. Rev. 46 (1–3) (2001) 3–26.
[17] D.F. Veber, S.R. Johnson, H.Y. Cheng, B.R. Smith, K.W. Ward, K.D. Kopple, Molecular properties that influence the oral bioavailability of drug candidates, J. Med. Chem. 45 (12) (2002) 2615–2623.
[18] R. Thomsen, M.H. Christensen, MolDock: a new technique for high-accuracy molecular docking, J. Med. Chem. 49 (11) (2006) 3315–3321.
[19] W.F. De Azevedo Jr., MolDock applied to structure-based virtual screening, Curr. Drug Targets 11 (3) (2010) 327–334.
[20] S. Sakkiah, K.W. Lee, Pharmacophore-based virtual screening and density functional theory approach to identifying novel butyrylcholinesterase inhibitors, Acta Pharmacol. Sin. 33 (7) (2012) 964–978.
[21] M. Wirth, V. Zoete, O. Michielin, W.H. Sauer, SwissBioisostere: a database of molecular replacements for ligand design, Nucleic Acids Res. 41 (Database issue) (2013) D1137–D1143.
[22] A.K. Debnath, Pharmacophore mapping of a series of 2,4-diamino-5-deazapteridine inhibitors of Mycobacterium avium complex dihydrofolate reductase, J. Med. Chem. 45 (1) (2002) 41–53.
[23] R. Kavitha, S. Karunagaran, S.S. Chandrabose, K.W. Lee, C. Meganathan, Pharmacophore modeling, virtual screening, molecular docking studies and density functional theory approaches to identify novel ketohexokinase (KHK) inhibitors, Biosystems 138 (2015) 39–52.
[24] A.N. Queiroz, B.A. Gomes, W.M. Moraes Jr., R.S. Borges, A theoretical antioxidant pharmacophore for resveratrol, Eur. J. Med. Chem. 44 (4) (2009) 1644–1649.
[25] L. Fang, Y. Pan, J.L. Muzyka, C.G. Zhan, Active site gating and substrate specificity of butyrylcholinesterase and acetylcholinesterase: insights from molecular dynamics simulations, J. Phys. Chem. B 115 (27) (2011) 8797–8805.
[26] M.A. Gordon, S.L. Chan, A.J. Trevor, Active-site determinations on forms of mammalian brain and eel acetylcholinesterase, Biochem. J. 157 (1) (1976) 69–76.
[27] S.N. Rao, M.S. Head, A. Kulkarni, J.M. LaLonde, Validation studies of the site-directed docking program LibDock, J. Chem. Inf. Model. 47 (6) (2007) 2159–2171.
[28] Q. Yu, N.H. Greig, H.W. Holloway, A. Brossi, Syntheses and anticholinesterase activities of (3aS)-N1, N8-bisnorphenserine, (3aS)-N1, N8-bisnorphysostigmine, their antipodal isomers, and other potential metabolites of phenserine, J. Med. Chem. 41 (13) (1998) 2371–2379.
[29] M. Rosini, V. Andrisano, M. Bartolini, M.L. Bolognesi, P. Hrelia, A. Minarini, A. Tarozzi, C. Melchiorre, Rational approach to discover multipotent anti-Alzheimer drugs, J. Med. Chem. 48 (2) (2005) 360–363.
[30] F. Prati, M. Bartolini, E. Simoni, A. De Simone, A. Pinto, V. Andrisano, M.L. Bolognesi, Quinones bearing non-steroidal anti-inflammatory fragments as multitarget ligands for Alzheimer's disease, Bioorg. Med. Chem. Lett. 23 (23) (2013) 6254–6258.
[31] A. Samadi, M. Estrada, C. Perez, M.I. Rodriguez-Franco, I. Iriepa, I. Moraleda, M. Chioua, J. Marco-Contelles, Pyridonepezils, new dual AChE inhibitors as potential drugs for the treatment of Alzheimer's disease: synthesis, biological assessment, and molecular modeling, Eur. J. Med. Chem. 57 (2012) 296–301.
[32] P.W. Elsinghorst, C.M. Tanarro, M. Gutschow, Novel heterobivalent tacrine derivatives as cholinesterase inhibitors with notable selectivity toward butyrylcholinesterase, J. Med. Chem. 49 (25) (2006) 7540–7544.
[33] G. Campiani, C. Fattorusso, S. Butini, A. Gaeta, M. Agnusdei, S. Gemma, M. Persico, B. Catalanotti, L. Savini, V. Nacci, E. Novellino, H.W. Holloway, N.H. Greig, T. Belinskaya, J.M. Fedorko, A. Saxena, Development of molecular probes for the identification of extra interaction sites in the mid-gorge and peripheral sites of butyrylcholinesterase (BuChE). Rational design of novel, selective, and highly potent BuChE inhibitors, J. Med. Chem. 48 (6) (2005) 1919–1929.
[34] P. Munoz-Ruiz, L. Rubio, E. Garcia-Palomero, I. Dorronsoro, M. del Monte-Millan, R. Valenzuela, P. Usan, C. de Austria, M. Bartolini, V. Andrisano, A. Bidon-Chanal, M. Orozco, F.J. Luque, M. Medina, A. Martinez, Design, synthesis, and biological evaluation of dual binding site acetylcholinesterase inhibitors: new disease-modifying agents for Alzheimer's disease, J. Med. Chem. 48 (23) (2005) 7223–7233.
[35] J.W. Sowell Sr., Y. Tang, M.J. Valli, J.M. Chapman Jr., L.A. Usher, C.M. Vaughan, J. W. Kosh, Synthesis and cholinergic properties of bis[[(dimethylamino)methyl] furanyl] analogues of ranitidine, J. Med. Chem. 35 (6) (1992) 1102–1108.
[36] A. Rampa, L. Piazzi, F. Belluti, S. Gobbi, A. Bisi, M. Bartolini, V. Andrisano, V. Cavrini, A. Cavalli, M. Recanatini, P. Valenti, Acetylcholinesterase inhibitors: SAR and kinetic studies on omega-[N-methyl-N-(3-alkylcarbamoyloxyphenyl) methyl]aminoalkoxyaryl derivatives, J. Med. Chem. 44 (23) (2001) 3810–3820.
[37] C. Galdeano, E. Viayna, I. Sola, X. Formosa, P. Camps, A. Badia, M.V. Clos, J. Relat, M. Ratia, M. Bartolini, F. Mancini, V. Andrisano, M. Salmona, C. Minguillon, G.C. Gonzalez-Munoz, M.I. Rodriguez-Franco, A. Bidon-Chanal, F.J. Luque, D. Munoz-Torrero, Huprine-tacrine heterodimers as anti-amyloidogenic compounds of potential interest against Alzheimer's and prion diseases, J. Med. Chem. 55 (2) (2012) 661–669.
[38] E. Nepovimova, E. Uliassi, J. Korabecny, L.E. Pena-Altamira, S. Samez, A. Pesaresi, G.E. Garcia, M. Bartolini, V. Andrisano, C. Bergamini, R. Fato, D. Lamba, M. Roberti, K. Kuca, B. Monti, M.L. Bolognesi, Multitarget drug design strategy: quinone-tacrine hybrids designed to block amyloid-beta aggregation and to exert anticholinesterase and antioxidant effects, J. Med. Chem. 57 (20) (2014) 8576–8589.
[39] M. Rosini, E. Simoni, M. Bartolini, A. Cavalli, L. Ceccarini, N. Pascu, D.W. McClymont, A. Tarozzi, M.L. Bolognesi, A. Minarini, V. Tumiatti, V. Andrisano, I. R. Mellor, C. Melchiorre, Inhibition of acetylcholinesterase, beta-amyloid aggregation, and NMDA receptors in Alzheimer's disease: a promising direction for the multi-target-directed ligands gold rush, J. Med. Chem. 51 (15) (2008) 4381–4384.
[40] M.L. Bolognesi, G. Chiriano, M. Bartolini, F. Mancini, G. Bottegoni, V. Maestri, S. Czvitkovich, M. Windisch, A. Cavalli, A. Minarini, M. Rosini, V. Tumiatti, V. Andrisano, C. Melchiorre, Synthesis of monomeric derivatives to probe memoquin's bivalent interactions, J. Med. Chem. 54 (24) (2011) 8299–8304.
[41] M.P. Arce, M.I. Rodriguez-Franco, G.C. Gonzalez-Munoz, C. Perez, B. Lopez, M. Villarroya, M.G. Lopez, A.G. Garcia, S. Conde, Neuroprotective and cholinergic properties of multifunctional glutamic acid derivatives for the treatment of Alzheimer's disease, J. Med. Chem. 52 (22) (2009) 7249–7257.

[42] Q. Yu, H.W. Holloway, T. Utsuki, A. Brossi, N.H. Greig, Synthesis of novel phenserine-based-selective inhibitors of butyrylcholinesterase for Alzheimer's disease, J. Med. Chem. 42 (10) (1999) 1855–1861.
[43] M.L. Bolognesi, R. Banzi, M. Bartolini, A. Cavalli, A. Tarozzi, V. Andrisano, A. Minarini, M. Rosini, V. Tumiatti, C. Bergamini, R. Fato, G. Lenaz, P. Hrelia, A. Cattaneo, M. Recanatini, C. Melchiorre, Novel class of quinone-bearing polyamines as multi-target-directed ligands to combat Alzheimer's disease, J. Med. Chem. 50 (20) (2007) 4882–4897.
[44] M.L. Bolognesi, M. Bartolini, M. Rosini, V. Andrisano, C. Melchiorre, Structure-activity relationships of memoquin: influence of the chain chirality in the multi-target mechanism of action, Bioorg. Med. Chem. Lett. 19 (15) (2009) 4312–4315.
[45] M.J. Valli, Y. Tang, J.W. Kosh, J.M. Chapman Jr., J.W. Sowell Sr., Synthesis and cholinergic properties of N-aryl-2-[[[5-[(dimethylamino)methyl]-2-furanyl] methyl]thio]ethylamino analogs of ranitidine, J. Med. Chem. 35 (17) (1992) 3141–3147.